

CHAPTER IV RESULTS AND DISCUSSION

4.1 Distillation Columns and Process Modeling

The gas separation plant unit I was modeled using the design data. The model was constructed for the unit operations within the battery limit. The ethane recovery case without Dew Point Control Unit (DPCU) condensate was chosen as a base case. The keyword-input file of this simulation model for the base case is summarized in Appendix A. The results from the simulation were in a good agreement with the design data as shown in Table 4.1. The stream properties results from simulation model are summarized in Appendix B. Product streams were chosen for illustration and are shown in Table 4.2. Distillation column operating parameters from simulation for demethanizer, deethanizer and depropanizer columns are shown in Figure 4.1 to 4.3, respectively. Therefore, this simulation model can be used to represent the process.

Table 4.1 The results from GSP I simulation model

Parameter	Simulation value
Composition	Simulation = Design \pm 0.001
Flowrate (mol/s)	Simulation \approx Design
Temperature (K)	Simulation = Design \pm 3 K
Pressure (barg)	Simulation \approx Design

4.2 Stand-alone Column Modifications

The Aspen Plus simulator version 11.1 has an advanced distillation feature that can analyze the distillation column performance. This feature can produce the CGCC for each column. The CGCC obtained were verified by comparing the condenser and reboiler duties with the simulation values.

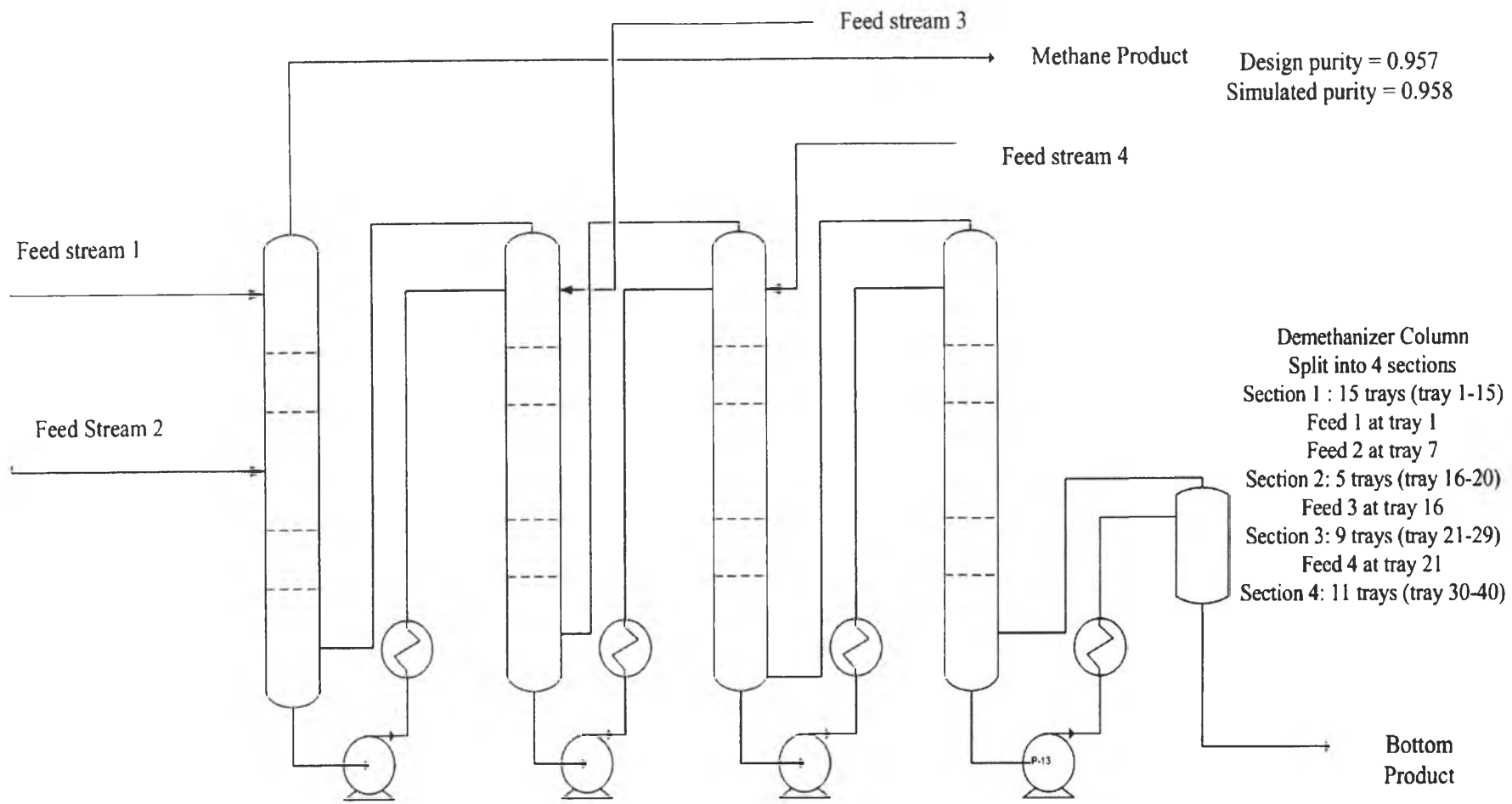


Figure 4.1 Aspen Plus simulation results of Demethanizer column.

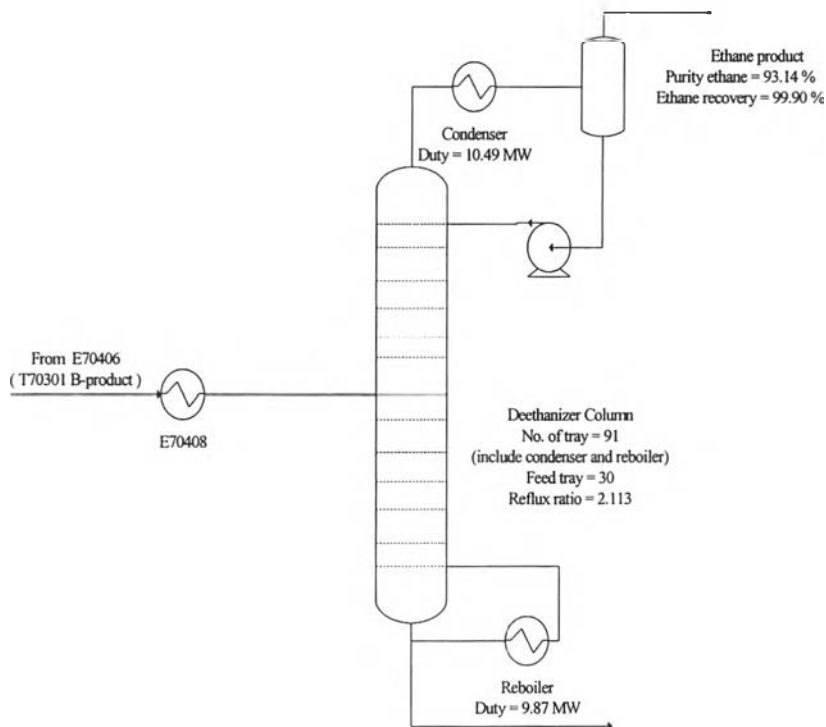


Figure 4.2 Aspen Plus simulation result for Deethanizer column.

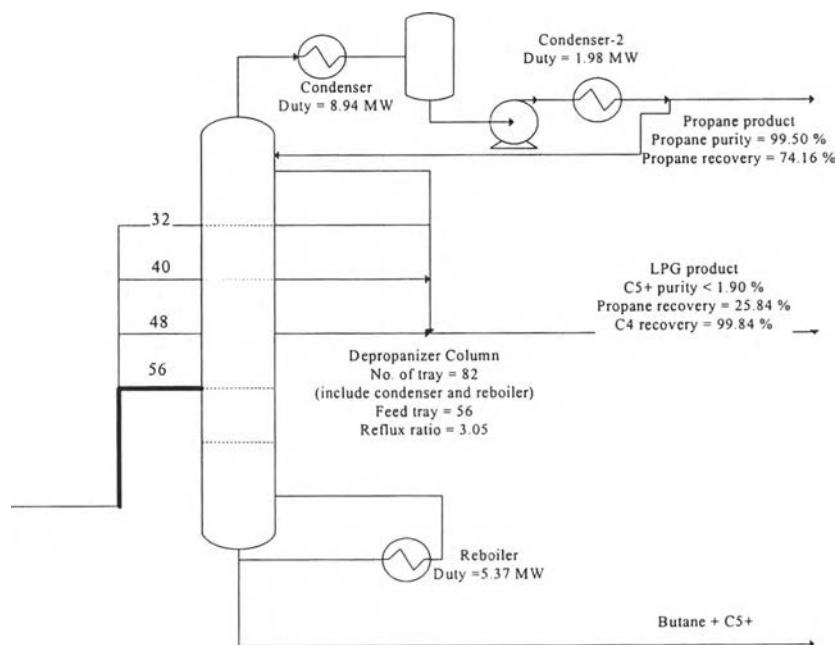


Figure 4.3 Aspen Plus simulation result for Depropanizer column.

Table 4.3 shows the comparison between the duty from the CGCC and simulations.

Table 4.2 Product stream composition and flow rate from the model

Component (mole fraction)	Methane Product	Ethane Product	Propane Product	LPG Product
N ₂	0.020	0.000	0.000	0.000
CH ₄	0.958	0.027	0.000	0.000
C ₂ H ₆	0.018	0.931	0.002	0.000
C ₃ H ₈	0.000	0.004	0.995	0.365
i-C ₄ H ₁₀	0.000	0.000	0.003	0.337
n-C ₄ H ₁₀	0.000	0.000	0.000	0.294
i-C ₅ H ₁₂	0.000	0.000	0.000	0.004
n-C ₅ H ₁₂	0.000	0.000	0.000	0.001
n-C ₆ H ₁₄	0.000	0.000	0.000	0.000
C 7 plus	0.000	0.000	0.000	0.000
CO ₂	0.004	0.038	0.000	0.000
Flow rate (mol/sec)	3385.559	404.554	172.300	158.141
Temperature (K)	171.900	273.300	300.000	300.000
Pressure (Bar)	15.000	27.700	16.500	16.500

Table 4.3 Comparison between condenser and reboiler loads from simulation and ones from CGCC

Column	Condenser load (MW)			Reboiler load (MW)		
	Simulation	CGCC	Error (%)	Simulation	CGCC	Error (%)
Demethanizer	-	-	-	0.31	0.31	0.00
Deethanizer	10.49	10.49	0.00	9.87	9.87	0.00
Depropanizer	10.92	10.92	0.00	5.37	5.37	0.00



4.2.1 Demethanizer column modifications

To generate CGCC, it is important to specify key components for the column. In this work, the key components were selected based on their relative volatility and column composition profile. The composition profile for the demethanizer column is shown in Figure 4.4.

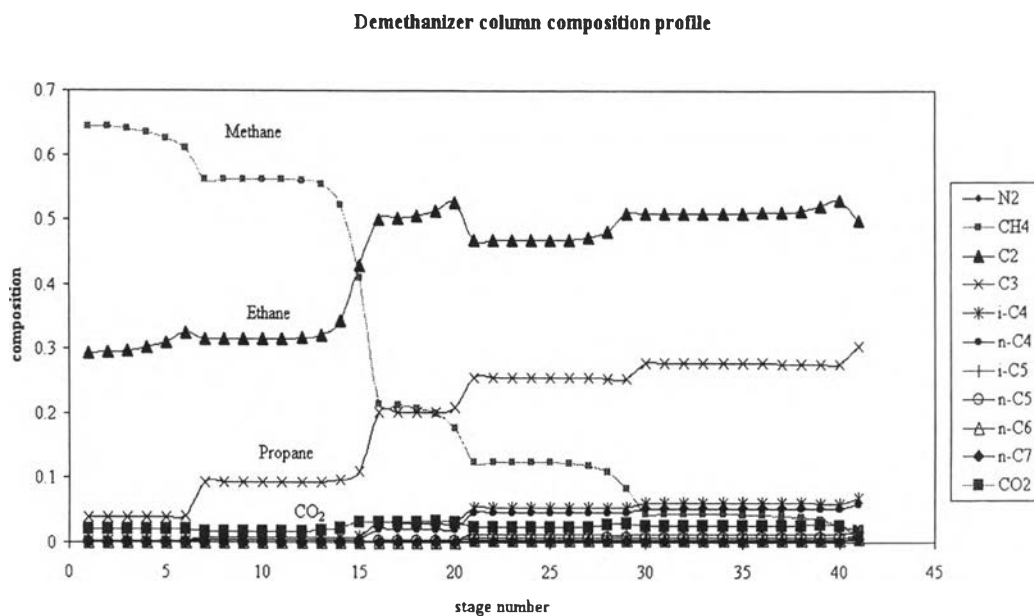


Figure 4.4 Demethanizer column composition profile.

Since the demethanizer column separates methane as an overhead product, methane and ethane should be the key components for this column. However, carbon dioxide which has its boiling point in between methane and propane are present. Therefore, it is necessary to classify CO₂, whether it is a light or heavy key component. From the separation principle, after ordering components by their boiling point, the light key component will be rich in the rectifying section, while the heavy key composition will be lean and vice versa in stripping section. From Figure 4.4, it can be seen that composition of methane and carbon dioxide is rich in the stage 1 to 15, while ethane composition is lean in the same range. This observation is based on the change in slope in composition profile. The rich

components are those having negative slope, while the lean components are those having positive slope. The components which are heavier than propane will not be grouped in heavy key component because their compositions are small and can be neglected in the calculation. Since propane composition is significant, it should be grouped with ethane as heavy key. Therefore, for stage 1 to 15, methane and carbon dioxide were grouped as light key, while ethane and propane were grouped as heavy key. The same idea was applied to stage 16-41 and methane was selected as light key, while carbon dioxide, ethane and propane were grouped as heavy key.

Demethanizer CGCC, was generated by specifying the key components as stated above, is shown in Figure 4.5. It can be seen that four pinch points were observed in demethanizer CGCC. Those four pinch points are corresponding to the location of four feed points. This agrees with the observation by many researchers (Dhole and Linnhoff, 1993; Bandyopadhyay *et al.*, 1998).

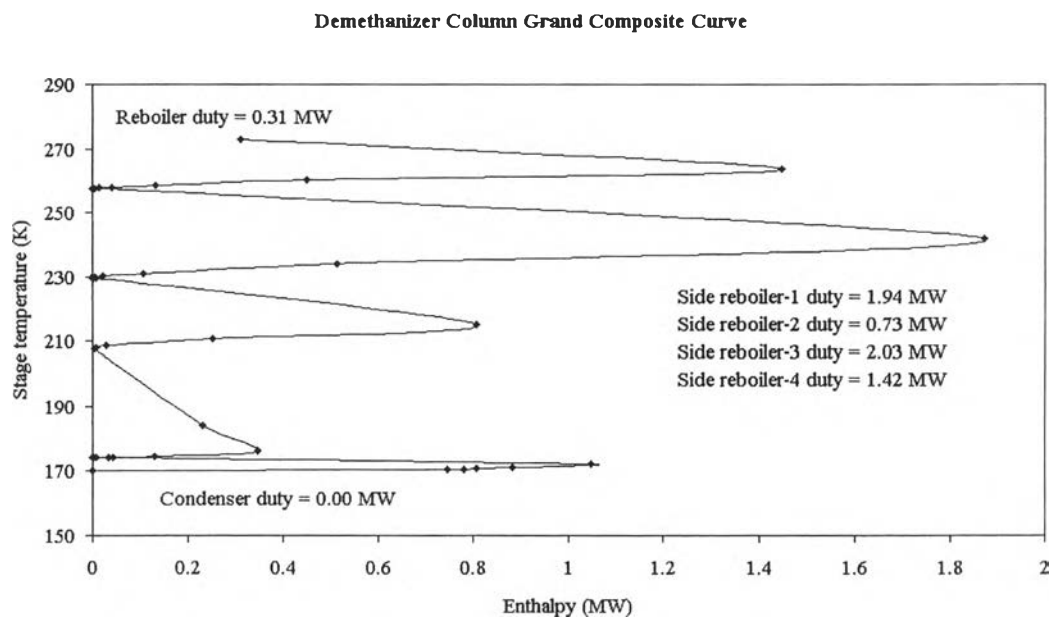


Figure 4.5 Demethanizer Column Grand Composite Curve.

From a guideline for column modification, the CGCC should be verified for energy loss gap to find a scope for reflux modification. From Figure 4.5,

there is no energy loss gap between CGCC and temperature axis, thus the column is already optimized, and no modification is required.

Another study is to verify that in terms of energy utilization, the use of side reboilers is better than the use of only one reboiler. This column operates with four side reboilers. The survey of the gas separation technology claims that this column arrangement is done in order to enhance the ethane recovery from natural gas and also reduce the duty of refrigeration unit. Therefore, the study was conducted in order to verify this claim. The study was conducted by modeling two kinds of demethanizer columns; one operating with side reboilers, and the other one operating without a side reboiler. The first column represents the actual column, while the latter column represents the column that operates by using just only main reboiler as shown in Figure 4.6 (a) and (b), respectively.

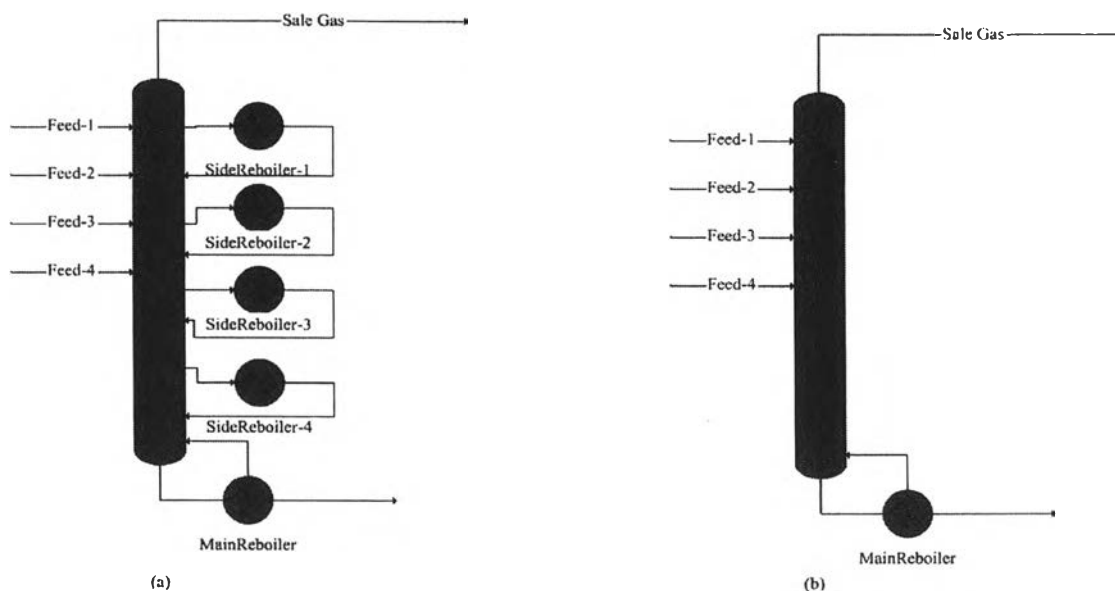


Figure 4.6 Demethanizer column configuration (a) column with side reboilers, (b) column without side reboiler.

The comparison between these two columns is shown in Table 4.4. It can be seen, from Table 4.4, that the main reboiler duty was reduced substantially when the side reboilers are employed. Thus, the use of side reboilers reduces main reboiler duty.

Table 4.4 Comparison of the duty of demethanizer column between the column without side reboilers and the one with side reboilers

Exchanger	Without side reboiler (MW)	With side reboiler (MW)
Side reboiler 1	-	1.94
Side reboiler 2	-	0.73
Side reboiler 3	-	2.03
Side reboiler 4	-	1.42
Main reboiler	6.52	0.31
Total	6.52	6.43

4.2.2 Deethanizer Column Modifications

Before generating deethanizer CGCC, the key components have to be specified first. The relative volatility and column composition profile were used for specifying key components. The column composition profile for deethanizer is shown in Figure 4.7.

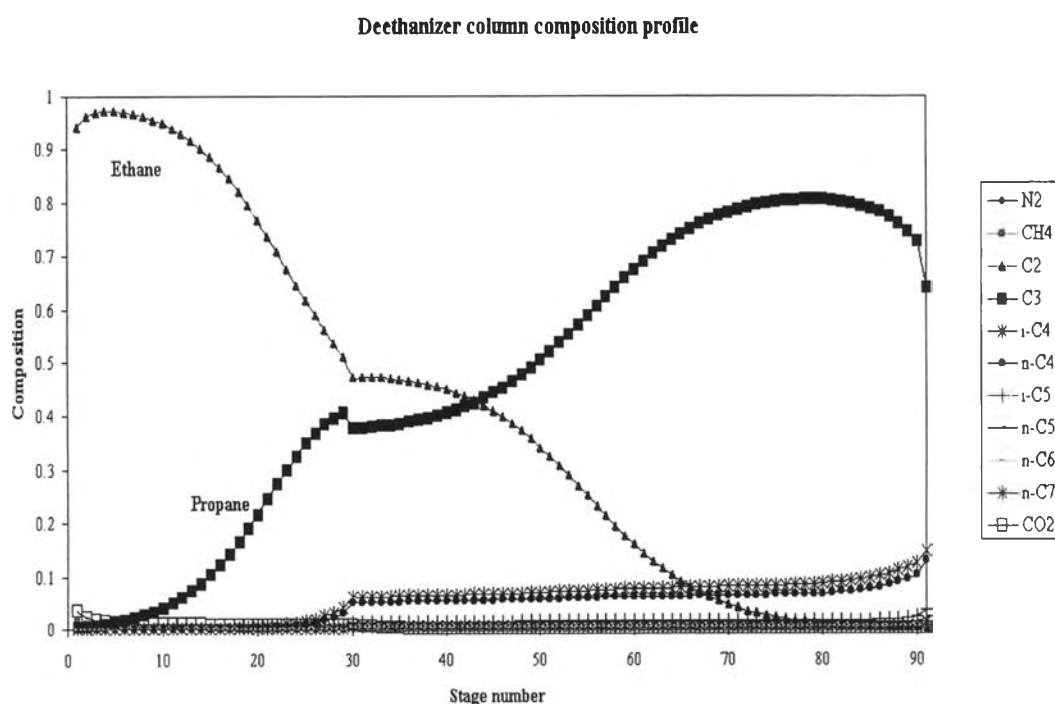


Figure 4.7 Deethanizer column composition profile.

The key component selection for this column applied the same idea as that was done in demethanizer column. For deethanizer column, it separates ethane out of the other components, therefore, ethane should be a light key and propane should be a heavy key. This agrees with the composition profile in Figure 4.7, ethane composition is rich in the rectifying section, while propane composition is lean and vice versa for stripping section. However, the components that are heavier than propane were not included in heavy keys because their composition is very small and can be negligible for the calculation. Therefore, ethane and propane were specified as light and heavy key, respectively.

The CGCC for deethanizer column, by specifying ethane as light key and propane as heavy key, is shown in Figure 4.8.

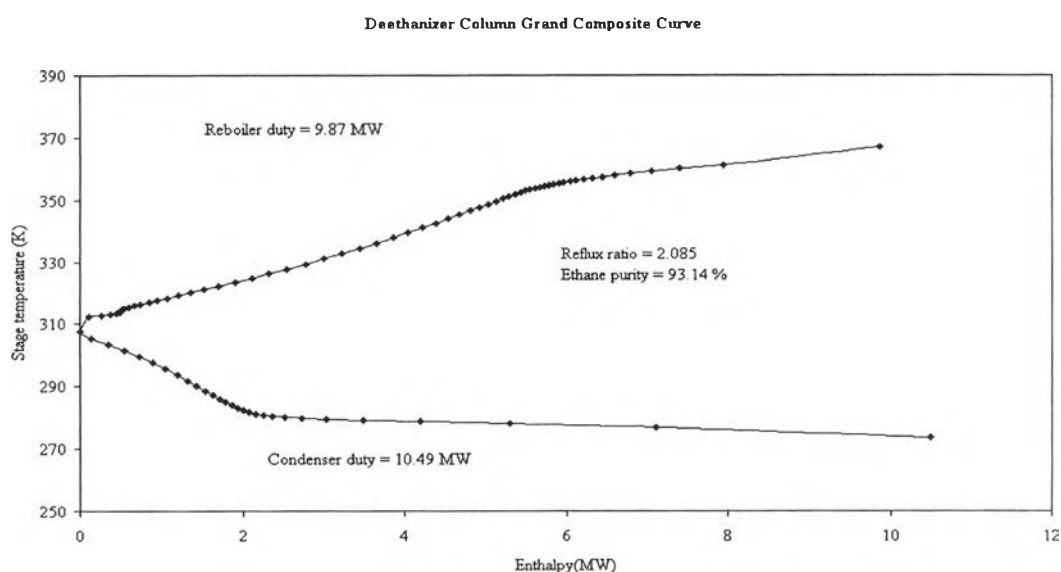


Figure 4.8 Deethanizer Column Grand Composite Curve.

From column modification guidelines, the CGCC should be verified for energy loss gap to find a scope for reflux modification. From Figure 4.8, deethanizer CGCC has a pinch point. The pinch point was observed at stage 30, which is the column feed stage. The location of pinch point is agreed well with the observation of many researchers (Dhole and Linnhoff, 1993; Bandyopadhyay *et al.*, 1998). However, in order to verify that the feed stage is already optimized. The

relationship between feed stage and ethane purity was conducted and the result is shown in Figure 4.9.

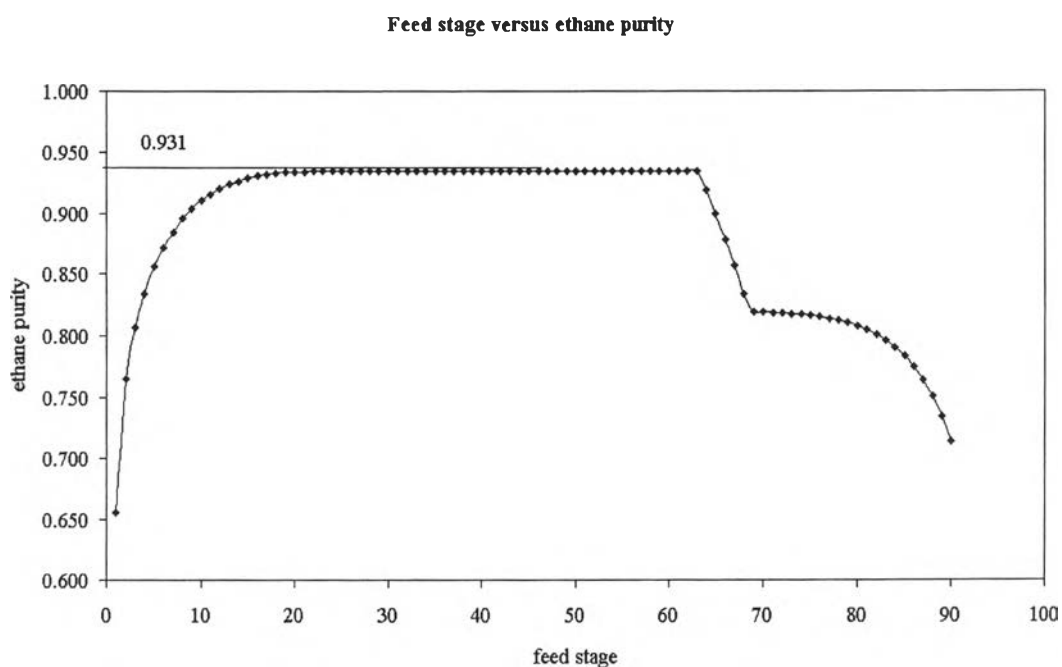


Figure 4.9 The relationships between ethane purity and feed stage of deethanizer column.

From Figure 4.9, it can be seen that if the column is fed in stage 21-63, the ethane purity will be maximum. In other word, the feed stage is in the optimum range. Therefore, the feed stage of this column (stage 30) is already optimized.

The CGCC in Figure 4.8 does not show the energy loss gap between the CGCC and vertical axis. Therefore, the column is already operated with optimum reflux. The relationships between the ethane purity and reflux ratio of deethanizer column were study to verify that the operating reflux is optimum. The result is shown in Figure 4.10.

It can be seen from Figure 4.10 that the ethane purity will be maximum at 0.931 when the reflux ratio of deethanizer column is greater than 2.085. Therefore, the operating reflux ratio (2.085) is already at the minimum value that can produce the required ethane specification.

After the energy loss gap was verified, the sharp enthalpy change near the pinch point would be verified next. If the sharp enthalpy changes were observed, the feed conditioning or side exchanger installation is required. Feed conditioning is preferred because it is easier to implement. From Figure 4.8, it can be seen that no sharp enthalpy changes near the pinch point. Therefore, the feed conditioning is not required.

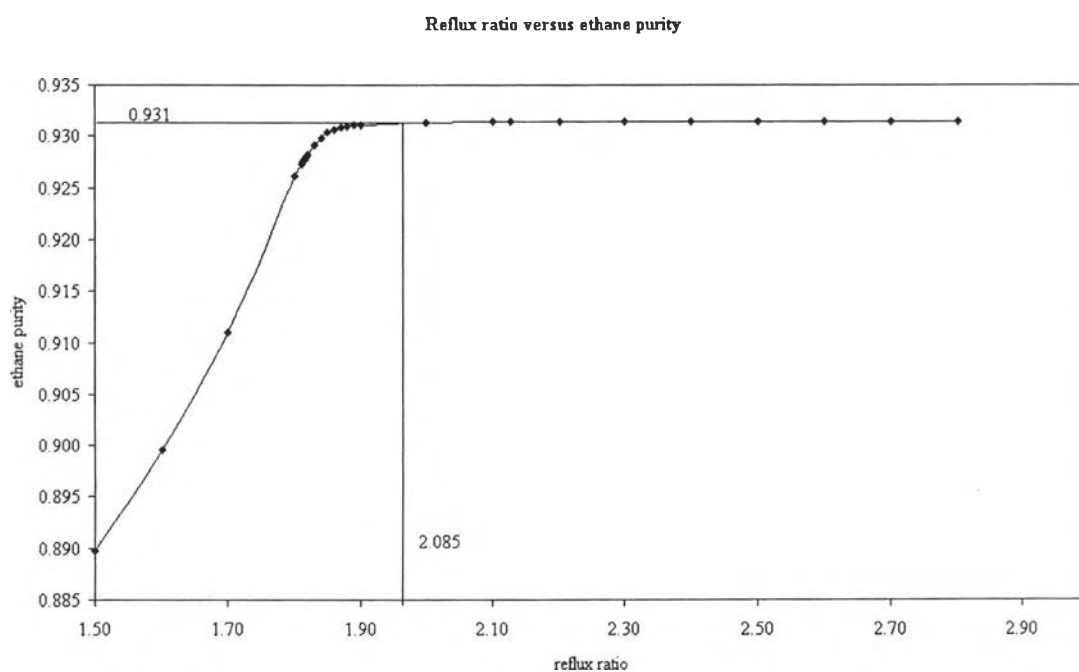


Figure 4.10 The relationships between ethane purity and reflux ratio of deethanizer column.

4.2.3 Depropanizer column modification

Before generating depropanizer CGCC, the key components have to be specified first. The column composition profile was used for specifying key components. The column composition profile for depropanizer is shown in Figure 4.11. From the separation principle, the light key composition will be rich in the rectifying section, while the heavy key composition will be lean and vice versa for stripping section. Since this column has side drawn stream at stage 41, therefore the key component specification should be specified separately into three sections.

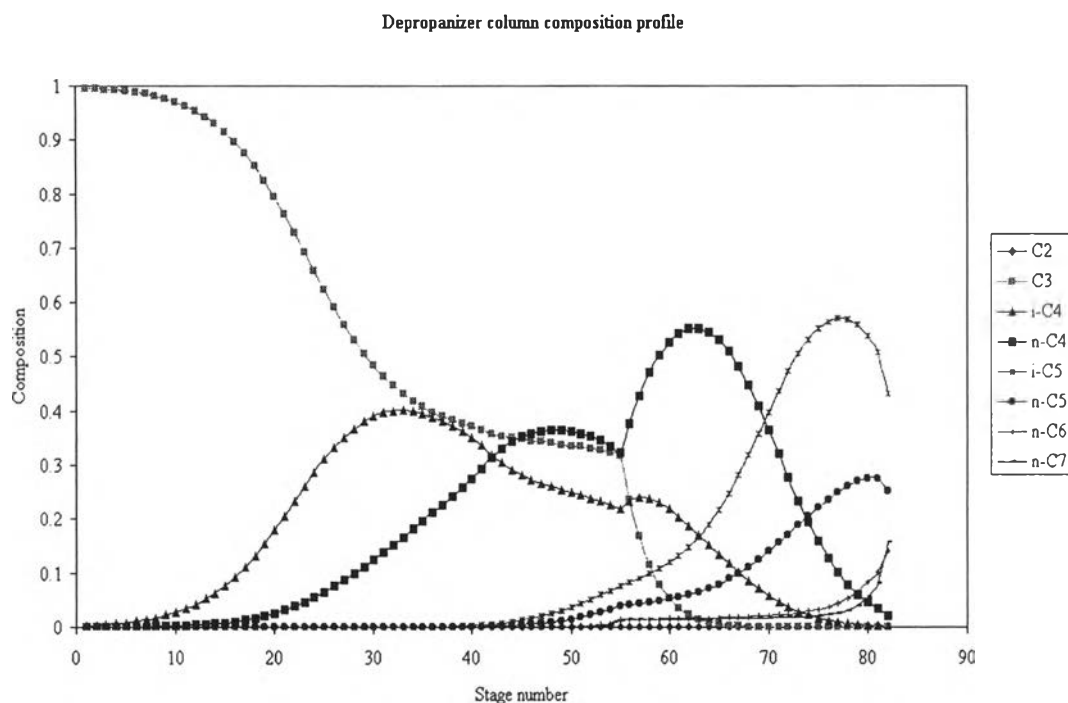


Figure 4.11 Depropanizer column composition profile.

From Figure 4.11, the first section starts from stage 1 to 50, the light key components are ethane and propane, and the heavy key components are iso-butane and the heavier. The second section starts from stage 51 to 55, the light key components are ethane, propane and iso-butane, and the heavy key components are n-butane and the heavier. The last section starts from stage 56 to 82, the light key components are ethane, propane, iso-butane and n-butane, and the heavy key components are iso-pentane and the heavier. The CGCC for this column is shown in Figure 4.12.

From Figure 4.12, the pinch point of this column was observed at stage 50. However, the operating feed stage is stage 56. Therefore, the relationship between product purity (propane purity) versus feed stage was studied in order to find the optimum feed stage. The result from the study is shown in Figure 4.13. The optimum feed stage should produce the maximum product purity. From Figure 4.13, it can be seen that the maximum propane purity is obtained when the feed stage is in the range of 21 to 82. Even though, the feed stage and the pinch point are not the

same, they are all in the range of the optimum feed stage. Therefore, the feed stage is already optimized.

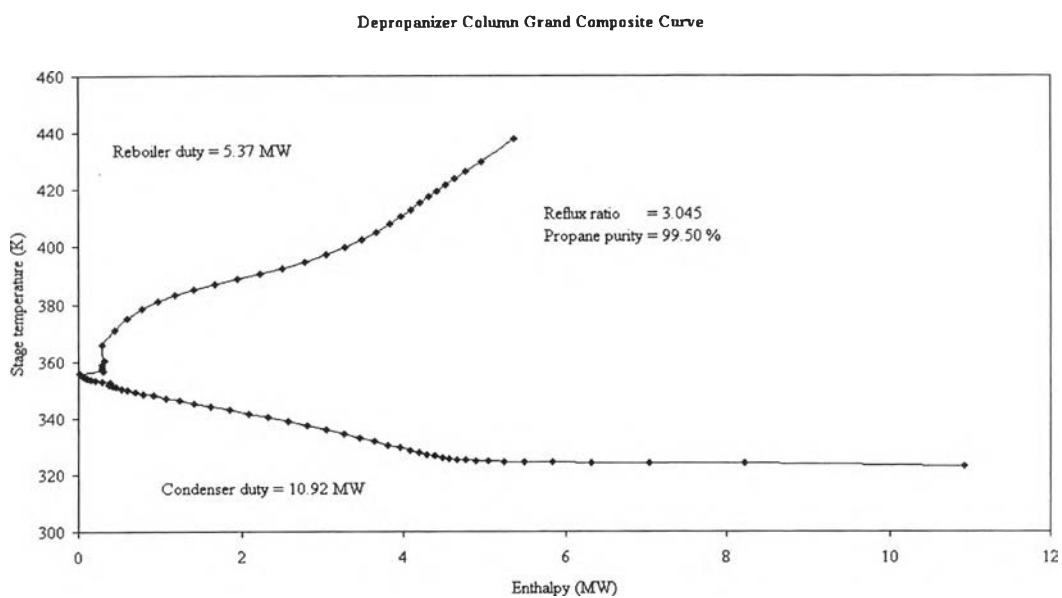


Figure 4.12 Depropanizer Column Grand Composite Curve.

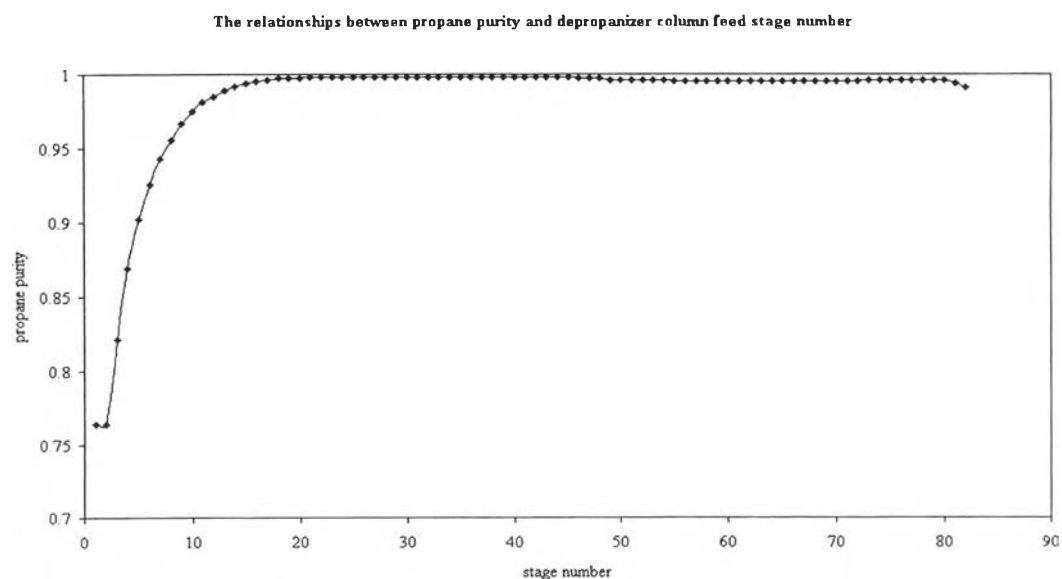


Figure 4.13 The relationships between propane purity and feed stage of depropanizer column.

From column modification guidelines, the CGCC should be verified for energy loss gap to find a scope for reflux modification. From Figure 4.12, no energy loss gap was observed from depropanizer CGCC. Therefore, the column is already optimized. However, the relationships between propane purity and reflux ratio of depropanizer column were studied to confirm that the operating reflux is already optimized. The result is shown in Figure 4.14

After the energy loss gap was verified, the sharp enthalpy change near the pinch point would be verified next. If the sharp enthalpy changes were observed, the feed conditioning or side exchanger installation is required. Feed conditioning is preferred because it is easier to implement. From Figure 4.12, it can be seen that no sharp enthalpy changes near the pinch point. Therefore, the feed conditioning is not required.

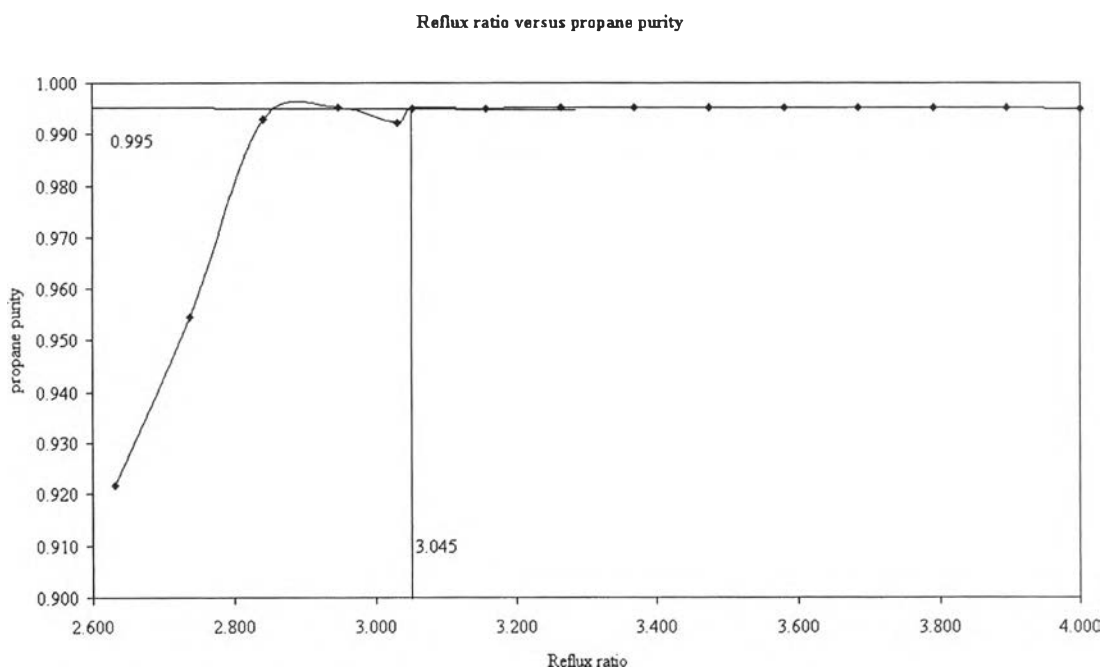


Figure 4.14 The relationships between propane purity and reflux ratio of depropanizer column.

4.3 Column integration

The energy saving potential for the process can be achieved more by identifying the potential for heat integration between distillation columns as shown in Figure 2.19. To identify the energy potential by column integration, the CGCC for each column will be plotted together on the same temperature-enthalpy diagram. In this study, the CGCC of demethanizer, deethanizer and depropanizer columns are plotted together in the same temperature-enthalpy diagram as shown in Figure 4.15.

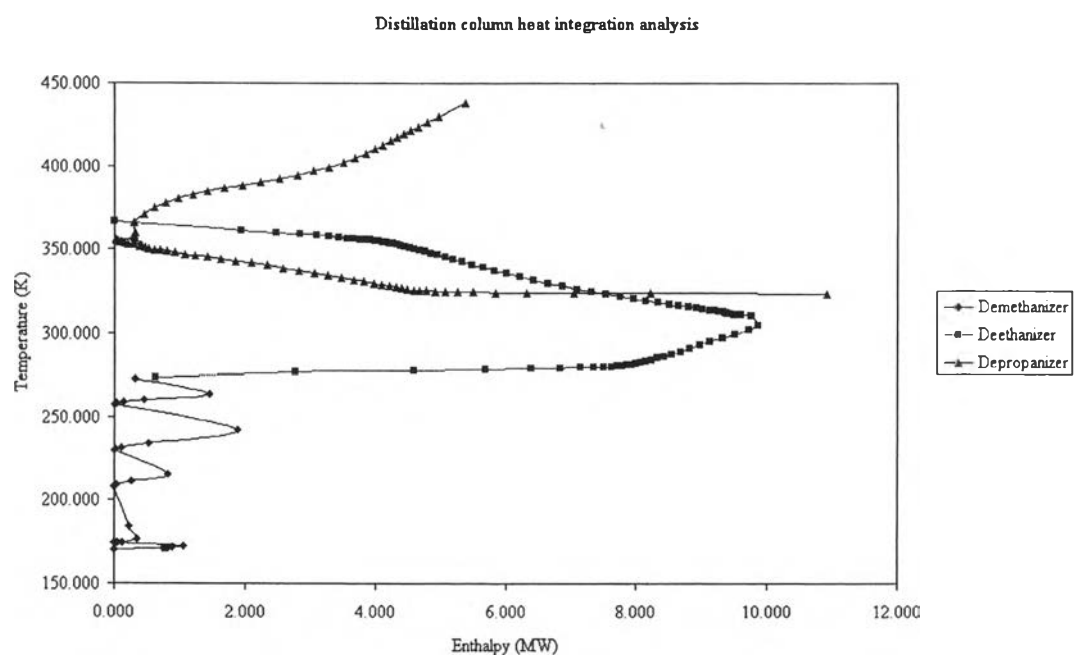


Figure 4.15 The study of distillation column heat integration.

It can be seen from Figure 4.15 that the column integration could be done between deethanizer and depropanizer column. However, the profile is still overlapping with each other. In order to make the column heat integration possible, two options were suggested and studied to see the feasibility in heat integration.

From Figure 4.15, the heat integration could be possible if

- (1) The CGCC of depropanizer is shifted upward. This can be done by increasing operating pressure of depropanizer column.
- (2) The CGCC of deethanizer is shifted downward. This can be done by decreasing operating pressure of deethanizer column.

The effect of the above two options were studied and the results were discussed as follows:

4.3.1 Increasing pressure of depropanizer column

First, the opportunity of heat integration by increasing pressure of depropanizer column was studied. The CGCC of depropanizer was shifted to higher temperature. However, this column cannot increase the pressure beyond 19 bar due to the material limitation. Therefore, the operating pressure of 18.5 bar was chosen for studied, the result showed that the condenser temperature of depropanizer (338.5 K) still lower than the reboiler temperature of deethanizer (366.4 K). Since the heat cannot be transferred from low temperature to high temperature, in other words, the heat removed from depropanizer condenser cannot be used to supply the heat of deethanizer reboiler. Thus, the heat integration between these two columns by increasing pressure of depropanizer column is not feasible.

4.3.2 Decreasing pressure of deethanizer column

Next, deethanizer pressure reduction was investigated. Since the overhead stream of deethanizer is cooled by refrigerant, which is available at -4.5°C (268.65 K). Thus, the pressure reduction in this column should not be reduced such that the overhead temperature is less than the refrigerant temperature.

In this study, it is not desirable to modify the existing equipments. Therefore, the result from the study should not require the modification of deethanizer condenser. This is feasible when the duty and UA of the condenser do not exceed those of the design. The condenser is designed for the duty and the UA value (product of overall heat transfer coefficient, U and heat transfer area, A) not greater than 10.99 MW and 1.64 MW/K (from equipment specification sheet of deethanizer condenser, PTT GSP I), respectively.

The result from this study is shown in Table 4.5. It can be seen that when the operating pressure was decreased, the condenser duty and UA are increased beyond the design values. The reason why the condenser duty load is increased when the pressure is decreased can be explained by the fact that when pressure is decreased, temperature is decreased. Since the heat of vaporization is increased

when the temperature is decreased; therefore, when the pressure is decreased, temperature will be decreased, resulting in the heat of vaporization increases. Therefore, the condenser duty is increased. Since the UA is calculated by dividing the duty by the temperature difference. When the pressure is decreased, the condenser duty increases, while temperature difference decreases. Therefore, the value of UA is increased.

Therefore, the pressure reduction of deethanizer column is not feasible. If this column pressure is not reduce, the reboiler temperature of this column is still greater than the overhead temperature of depropanizer column, which implies that the column heat integration by reducing pressure of deethanizer column is not appropriate.

Table 4.5 Effect of deethanizer pressure reduction on condenser duty

Pressure (barg)	26.00	27.00	28.00	28.50	29.00
Inlet temperature (K)	274.68	276.18	277.65	278.37	279.08
Outlet temperature (K)	269.82	271.48	273.09	273.89	274.68
Coolant inlet temperature (K)	268.65	268.65	268.65	268.65	268.65
Coolant outlet temperature (K)	268.65	268.65	268.65	268.65	268.65
Condenser duty (MW)	11.12	10.85	10.58	10.44	10.31
LMTD (K)	2.96	4.80	6.46	7.25	8.03
UA (MW/K)	3.76	2.26	1.64	1.44	1.28

The study of two options for column integration shows that neither pressure reduction in deethanizer column nor pressure increasing in depropanizer column can open up the opportunity for column integration. Thus, the column integration is not appropriate for energy optimization in this system.

4.4 Pinch Analysis

4.4.1 Data extraction

After the column optimization was completed, now the heating and cooling requirement for each stream is known. So, the first step in pinch analysis is begun. The stream data, together with the network information from Aspen Plus are transferred to Aspen Pinch program. The hot and cold streams are selected based on the process flowsheet. In this study, eight hot and eight cold streams were selected. The location and information of each stream in process flowsheet are shown in Figure 4.16 and Table 4.6, respectively.

The minimum temperature difference was pre-optimized based on the cost of the network. The relationship between the utility, capital and total cost of the network at various values of ΔT_{\min} is shown in Figure 4.17.

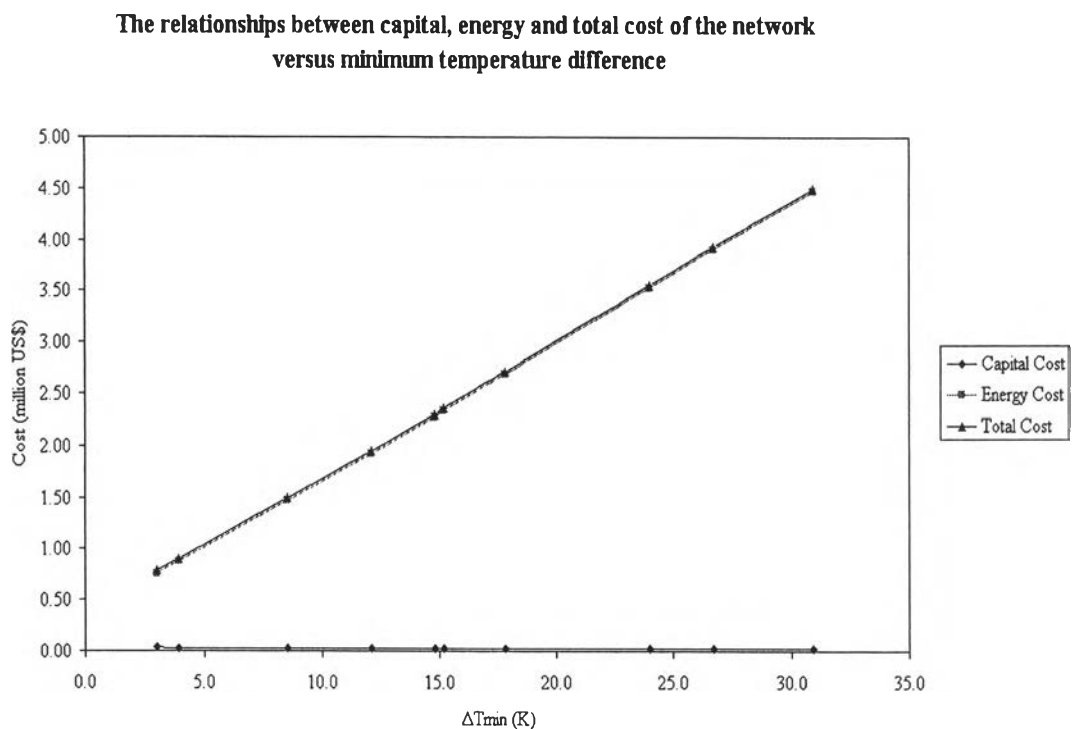


Figure 4.17 The relationships between capital, operating and total cost of the network as a function of ΔT_{\min} .

It can be seen that the total cost of the network was dominated by the utility cost. It can be seen also that the utility cost is proportional to the value of ΔT_{\min} . This implies that using a small value of ΔT_{\min} , the network cost will be small.

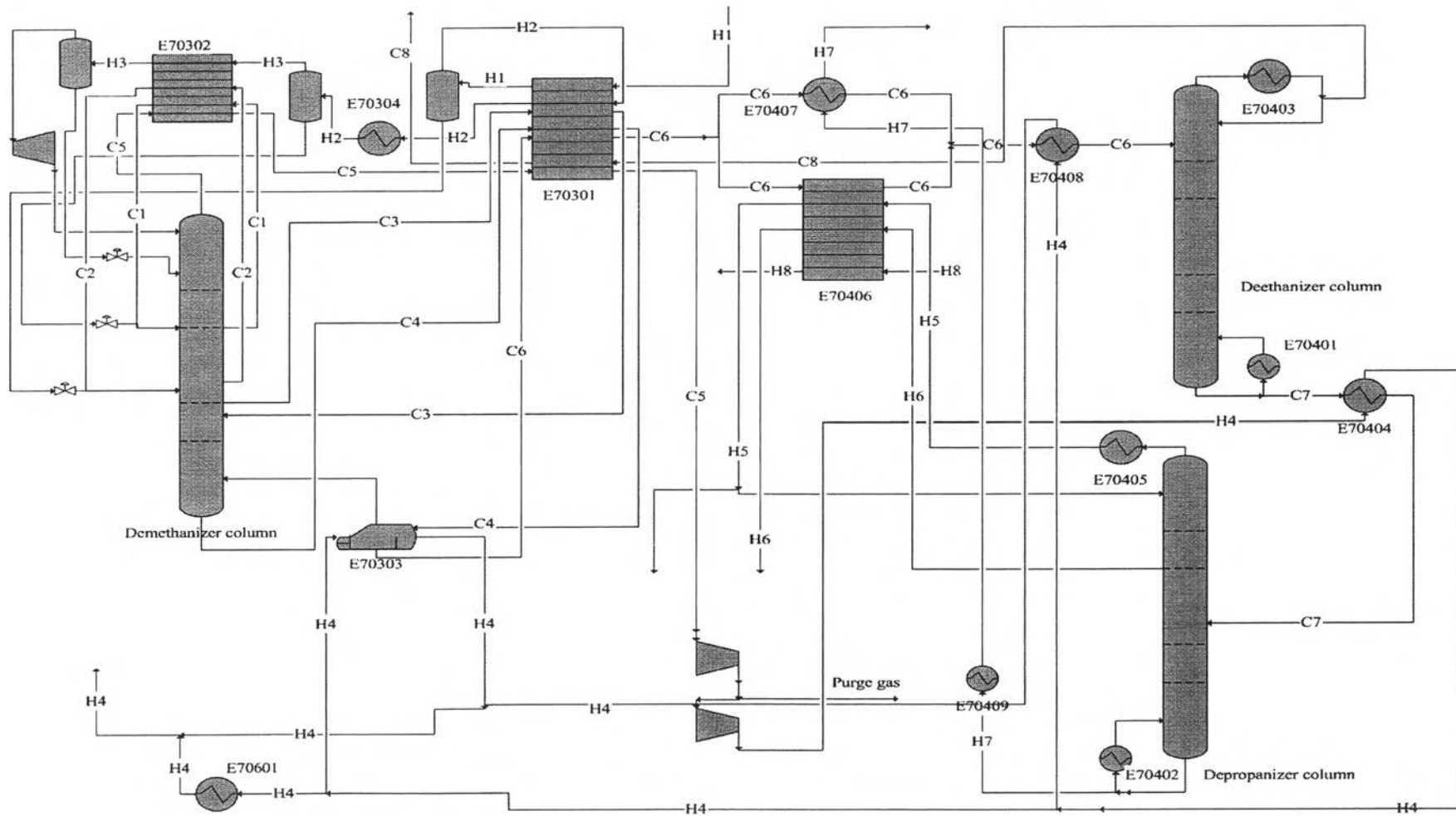


Figure 4.16 Location of hot and cold streams in process flowsheet of gas separation plant I.

Table 4.6 Stream information for pinch analysis (Hot streams)

Stream ID	Supply Temperature (K)	Target Temperature (K)	Stream Duty (MW)	Heat capacity flowrate (MW/K)	Heat transfer coefficient (kW/m ² .K)	Pressure (barg)	Description
H1	295.50	255.00	11.85	0.29	0.66	43.10	Feed to 255K separator
H2	255.00	233.00	6.98	0.32	0.65	42.90	Feed to 233K separator
H3	233.00	204.50	17.96	0.39	0.88	42.70	Feed to expander
H4	398.15	322.22	10.72	0.14	2.13	44.60	Sale gas product
H5	319.98	300.00	1.34	0.07	1.30	16.50	Depropanizer reflux stream
H6	347.69	300.00	1.12	0.02	0.91	16.00	LPG product
H7	435.28	300.00	0.85	0.01	0.37	16.00	Natural gasoline product
H8	313.00	300.00	1.06	0.08	1.20	19.00	Refrigerant at 19 barg

(Cont.)

Table 4.6 (Continued) Stream information for pinch analysis (Cold streams)

Stream ID	Supply Temperature (K)	Target Temperature (K)	Stream Duty (MW)	Heat capacity flowrate (MW/K)	Heat transfer coefficient (kW/m ² .K)	Pressure (barg)	Description
C1	192.12	210.91	1.88	0.10	1.47	15.00	Demethanizer side stream-1
C2	219.81	228.29	0.76	0.09	1.38	15.00	Demethanizer side stream-2
C3	247.30	259.59	2.05	0.17	0.70	15.00	Demethanizer side stream-3
C4	265.79	273.29	1.79	0.24	1.62	15.00	Demethanizer reboiler stream
C5	170.34	287.35	15.35	0.13	0.32	17.90	Methane feed to sale gas compressor
C6	274.64	316.10	16.47	0.14	1.92	28.00	Deethanizer column feed
C7	341.16	361.42	1.94	0.10	1.96	16.50	Depropanizer column feed
C8	240.83	287.35	5.11	0.11	0.55	11.00	Ethane product

The relationship between the energy consumption and ΔT_{\min} was also studied. The result is shown in Figure 4.18.

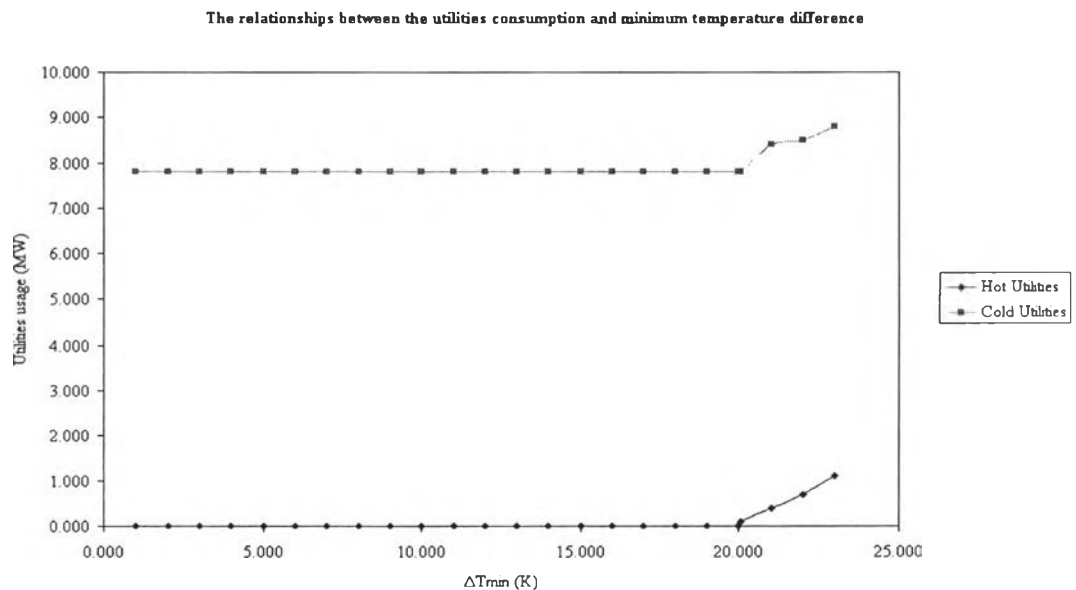


Figure 4.18 The relationships between hot and cold utility requirement at various ΔT_{\min} .

It can be seen that at ΔT_{\min} less than 20.05 K, there is no hot utility consumption and the cold utility consumption is constant. From this observation, the problem is called threshold problem, when ΔT_{\min} is less than 20.05 K. For threshold problem, there is only one type of utility that is required in the process when ΔT_{\min} is less than $\Delta T_{\min, \text{threshold}}$. Therefore, the GSP I requires only one kind of utility (cold utility) when ΔT_{\min} is less than 20.05 K. Since the value of temperature difference for the existing heat exchangers is in the range of 2-22 K as shown in Table 4.7. In order to make a little change on network configuration, the minimum temperature difference for the network should be the minimum temperature difference among heat exchangers. From Table 4.7, it can be seen that the minimum temperature difference is 2.05 K at heat exchanger E70304. Therefore, the appropriate value of ΔT_{\min} for this study is 2 K.

Table 4.7 Heat exchangers design specification data.

Exchanger	Duty (MW)	Area (m ²)	UA (W/K)	ΔT_{\min} (K)
Coldbox1	16.295	10083.600	2.385	2.720
Coldbox2	10.334	5283.000	0.876	4.710
Coldbox3	3.665	1918.700	0.528	2.920
E70303	1.395	76.100	0.036	10.700
E70304	2.420	1539.000	0.534	2.050
E70404	4.640	534.000	0.170	21.700
E70407	0.221	121.200	0.020	10.000
E70408	1.337	145.000	0.049	13.600
E70409	1.560	134.000	0.034	11.000
E70601	8.450	510.000	0.224	14.000

4.4.2 Performance targeting

Composite curves of process streams at $\Delta T_{\min} = 2.00$ and 20.05 K are shown in Figure 4.19 and 4.20, respectively. It can be seen from Figure 4.19 that the hot and cold composite curves are separated by temperature difference more than 2 K, i.e. temperature difference is greater than ΔT_{\min} , thus no pinch point can be observed from composite curves. In other words, when the problem is threshold, the pinch point cannot be observed from the composite curves. However, at the threshold temperature difference, the pinch point is observed as shown by dashed line in Figure 4.20. At that point, hot and cold composite curves are separated by temperature difference of 20.05 K. Therefore, the pinch point can be observed by composite curves when ΔT_{\min} is less than $\Delta T_{\min, \text{threshold}}$. Since $\Delta T_{\min} = 2$ K, was used in this study; therefore, the process streams require only cooling utilities to complete the process requirement.

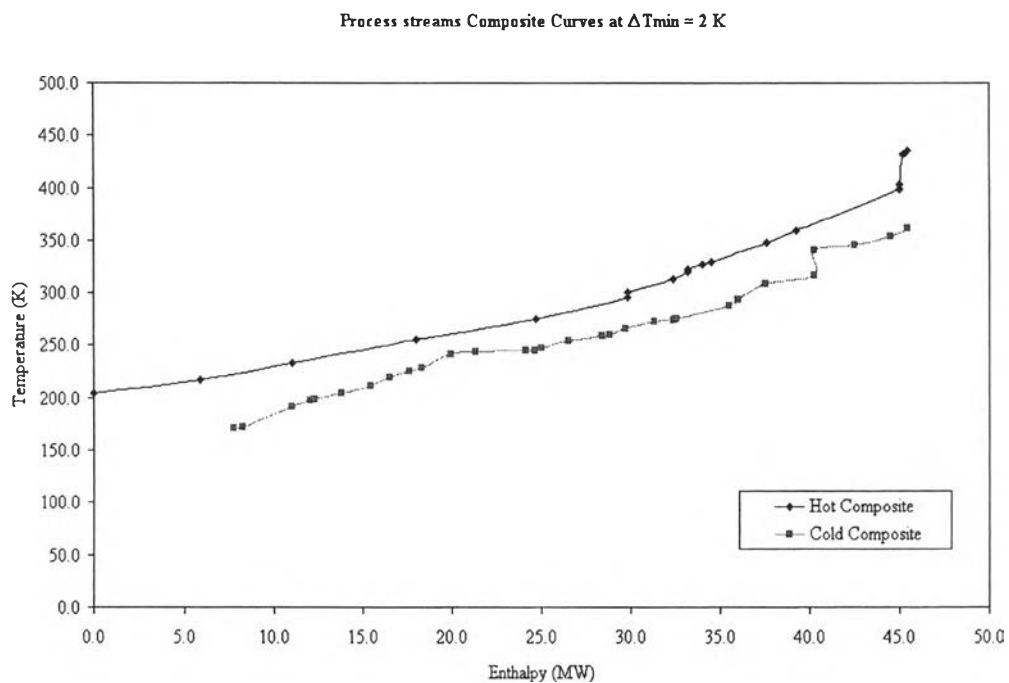


Figure 4.19 Process streams composite curves at $\Delta T_{\min} = 2 \text{ K}$.

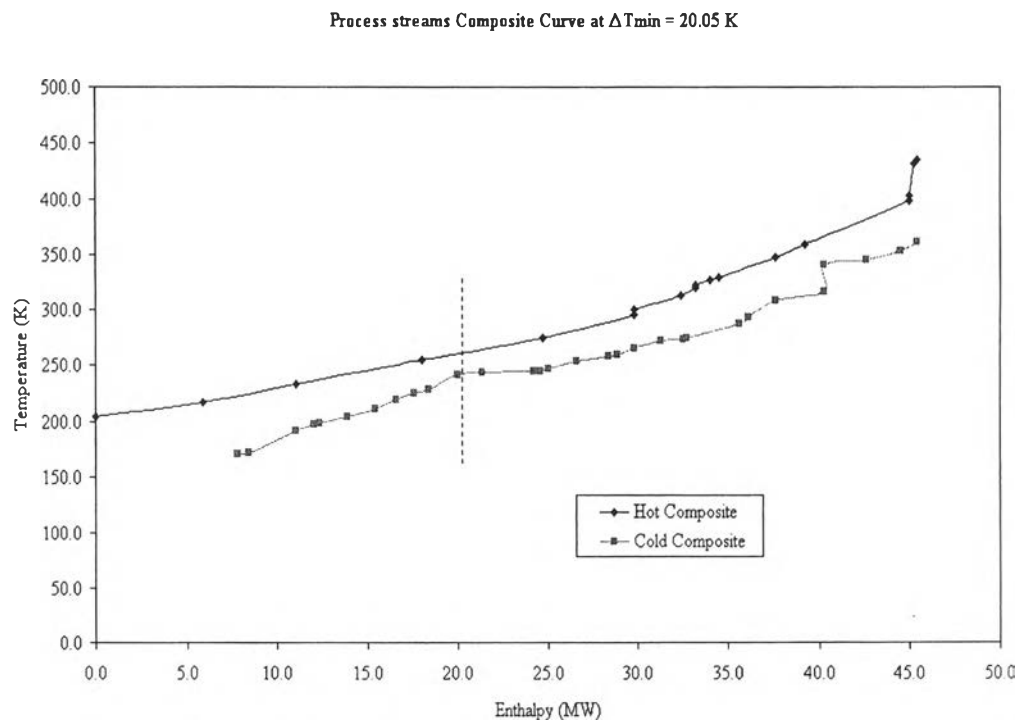


Figure 4.20 Process streams composite curves at $\Delta T_{\min} = 20.05 \text{ K}$.

The process grand composite curve at $\Delta T_{\min} = 2$ K is shown in Figure 4.21. It can be seen from Figure 4.19 and 4.21 that the heating and cooling requirement to complete the process requirement are 0.00 and 7.80 MW, respectively.

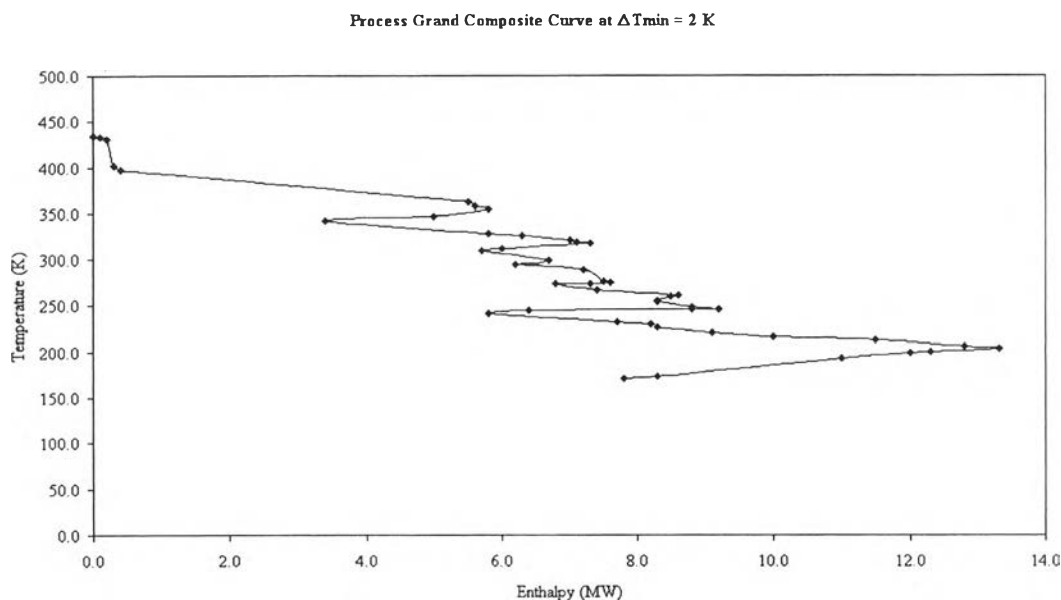


Figure 4.21 Process grand composite curve at $\Delta T_{\min} = 2$ K.

The overall energy saving of the process can be investigated further by analyzing the heat integration between process streams and distillation columns. The analysis was done by plotting the process grand composite curve at $\Delta T_{\min} = 2$ K and three column grand composite curves, i.e. demethanizer, deethanizer and depropanizer CGCC, on the same temperature-enthalpy plot as shown in Figure 4.22. The heat integration between process streams and distillation column will be beneficial if the columns are placed on either side of the process pinch point without overlapping with each other, i.e. the column should be placed on either entirely above or below pinch. From Figure 4.22, it can be seen that the profile of the process streams and the CGCCs are crossing with each other, which shows infeasible heat transfer. Therefore, the heat integration between the process streams and distillation columns is not appropriate.

The current energy usage from the design specification is 0.00 and 12.18 MW for hot and cold utility, respectively. The comparison between the current energy usage and the minimum energy requirement is shown in Table 4.8. It can be seen that the current energy usage is 56.15 % greater than the minimum value, which suggests the room for modification. The corresponding energy cost saving, which was calculated based on the refrigerant cost, is US\$ 1,362,092.40 / yr.

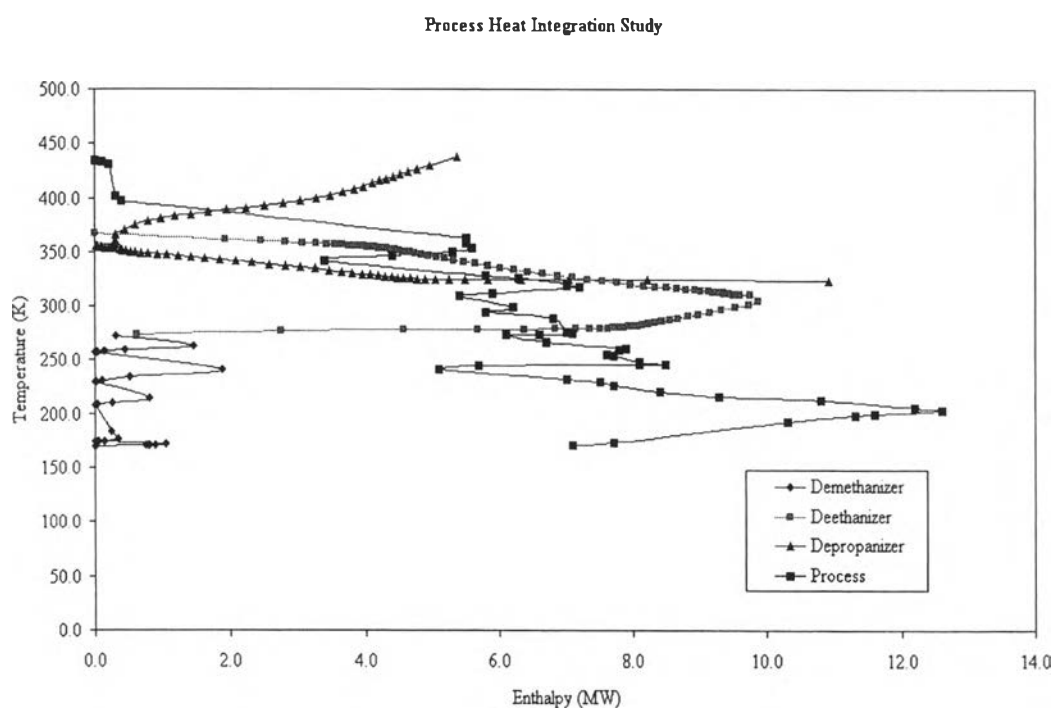


Figure 4.22 Process heat integration analysis between process streams and distillation column.

Table 4.8 Comparison between current and minimum energy consumption

Utility type	Current energy consumption (MW)	Minimum energy consumption (MW)	Percentage excess energy usage
Hot utility	0.00	0.00	0.00
Cold utility	12.18	7.80	56.15

The target for capital investment was predicted by Aspen Pinch program. The minimum number of heat exchangers and heat transfer area for the network was predicted to be 15 units and 15,912.5 m², respectively for the new network, which is corresponding to capital investment of US\$ 251,280.10. Since the objective of this work is to modify the existing heat exchanger network for improving energy usage, the existing area will be re-used as much as possible. Since the existing heat transfer area for the network is 20,344.6 m², which is greater than the minimum area requirement for the new network (15,912.5 m²); thus no capital investment is required for the modification.

In summary, the modification does not require the investment but it results in energy cost saving of US\$ 1,362,092.40 / yr.

4.4.3 Heat exchanger network modifications

The heat exchanger network design or modification is usually done on grid diagram because of its simplicity. In this study, the heat exchanger network modifications were also done on grid diagram. The existing heat exchanger network configuration is shown in Figure 4.23. It was shown in section 4.4.2 that the process has no pinch point; therefore, no pinch separation was observed in grid diagram. The heat exchanger network modification was done following the pinch principle. Since the process has no pinch point, i.e. threshold problem; therefore, the network can be designed freely. In process modification, it is desirable to design a network configuration as closed as the existing network. Thus, the modification was done in order to achieve the minimum change of the existing configuration. From Figure 4.23, it can be seen that streams C6 and C7 outlet temperatures do not reach their targets as indicated by dotted line. For stream C6, the outlet temperature should be 316.1 K; however, the outlet temperature from E70408 is just 314.5 K. Same as stream C6, the outlet temperature of stream C7 should be 361.4 K; however, the outlet temperature from E70404A is just 351.7 K. Therefore, the modifications on process condition are required to bring these streams to their target temperatures. This was done by adjusting outlet temperature of stream H4 from 371.1 K to 361.9 K. The resulting modified network is shown in Figure 4.24. The heat exchanger operating condition is summarized in Table 4.9.

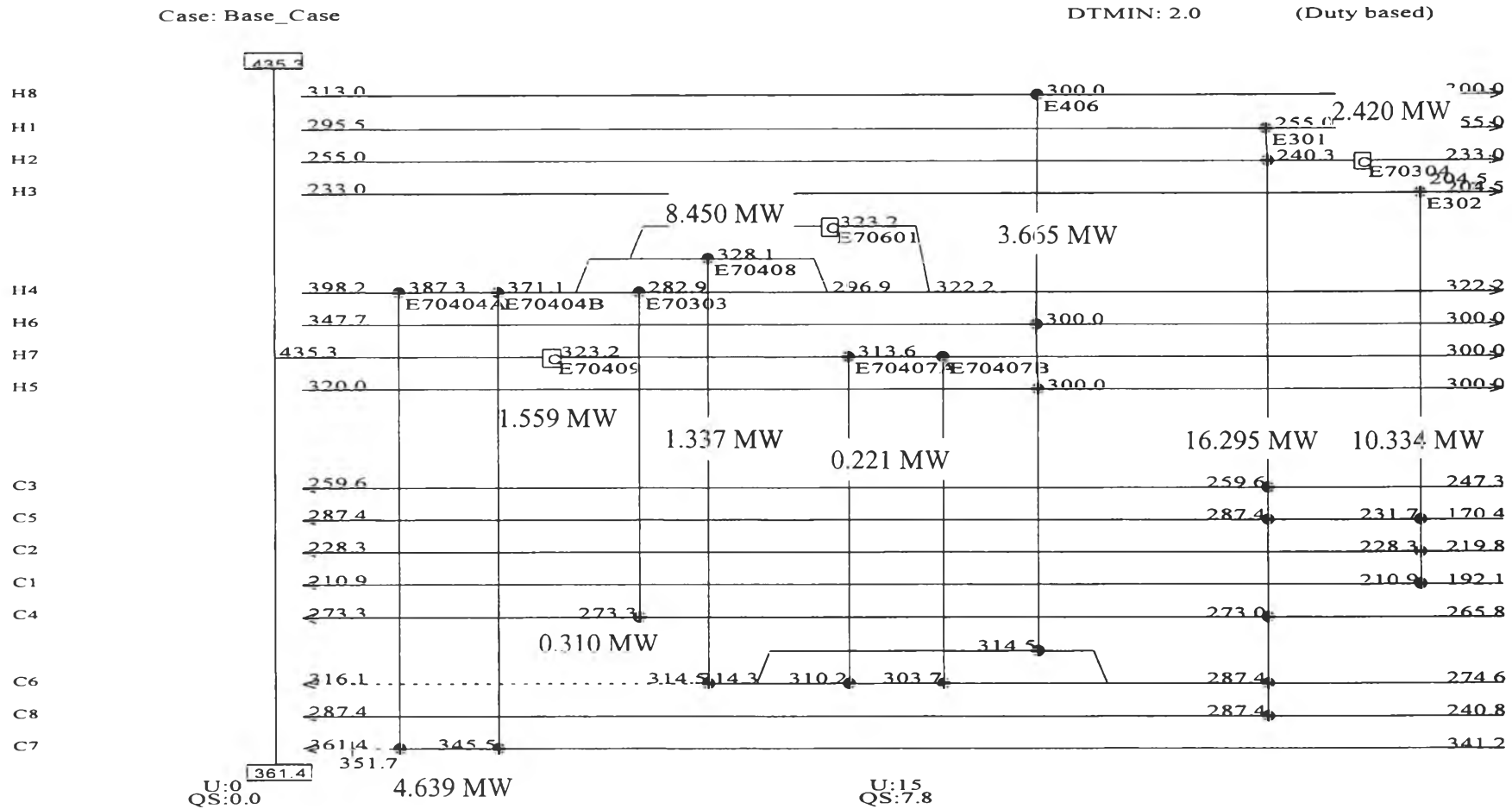


Figure 4.23 Grid diagram for the existing heat exchanger network configuration (Base case grid diagram).

Case: ExistingOption_1

DTMIN: 2.0

(Duty based)

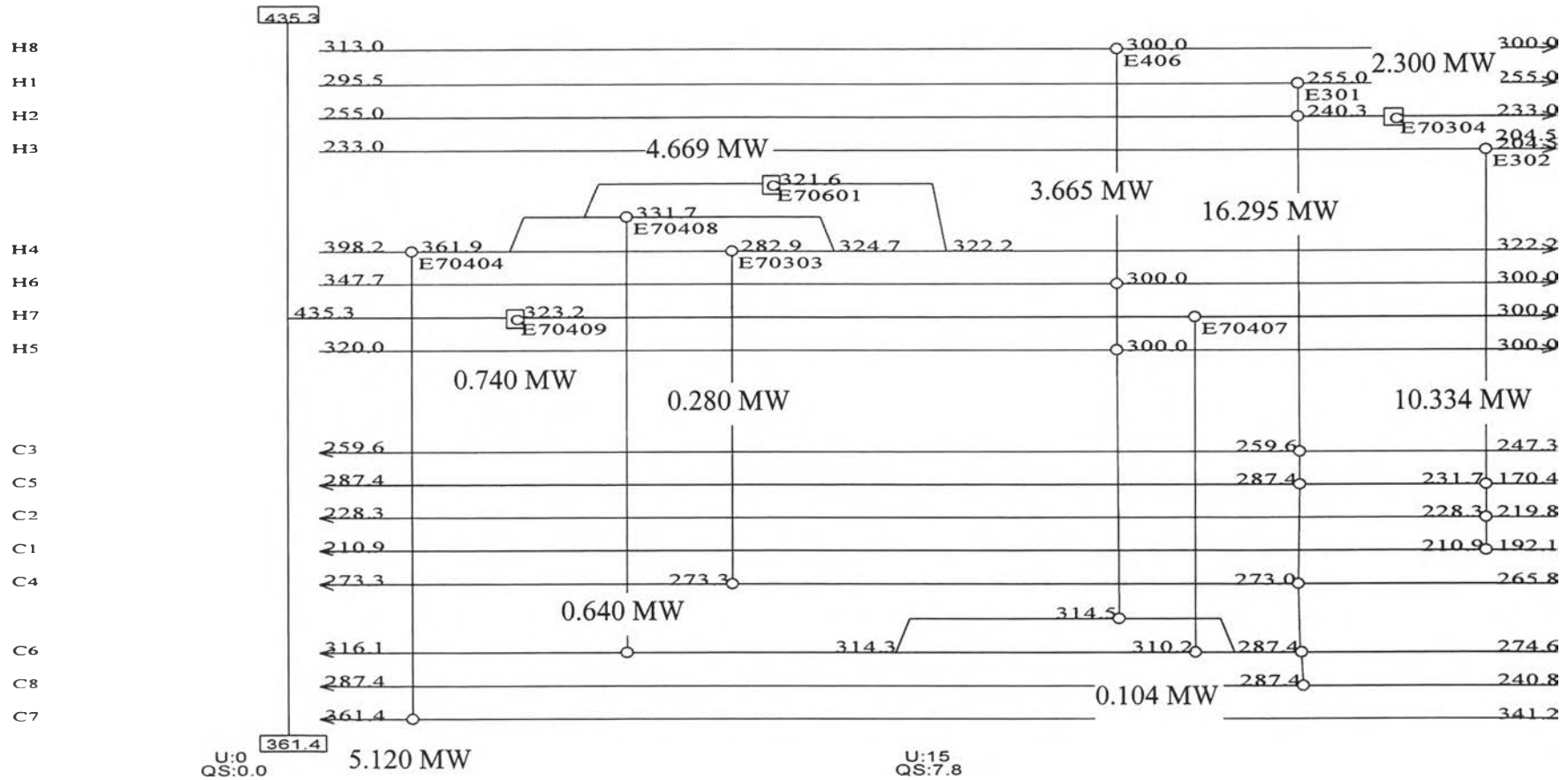


Figure 4.24 Grid diagram for heat exchanger network modification

Table 4.9 Operating conditions for existing and modified heat exchanger network

Existing network

Heat exchanger	Hot side		Cold side		Duty (MW)
	T _{in} (K)	T _{out} (K)	T _{in} (K)	T _{out} (K)	
E70303	370.63	282.15	272.98	273.29	0.31
E70304*	239.50	233.00	230.95	230.95	2.42
E70404	398.15	370.63	341.20	368.65	4.64
E70407	323.15	300.00	287.35	313.15	0.22
E70408	370.63	328.15	313.50	316.10	1.34
E70409**	435.28	323.15	312.15	318.15	1.56
E70601**	398.15	322.15	308.15	318.15	8.45

Modified network

Heat exchanger	Hot side		Cold side		Duty (MW)
	T _{in} (K)	T _{out} (K)	T _{in} (K)	T _{out} (K)	
E70303	<i>361.90</i>	<i>282.90</i>	272.98	273.29	0.28
E70304*	<i>240.30</i>	233.00	230.95	230.95	2.30
E70404	398.15	<i>361.90</i>	341.20	<i>361.42</i>	5.12
E70407	323.15	300.00	287.35	<i>310.20</i>	0.10
E70408	<i>361.90</i>	<i>331.70</i>	<i>314.30</i>	316.10	0.64
E70409**	435.28	323.15	312.15	318.15	0.74
E70601**	<i>361.90</i>	<i>321.60</i>	308.15	318.15	4.69

(Italicized numbers indicated modified conditions)

* Utility exchangers. Propylene refrigerant is used as cooling media.

** Utility exchangers. Cooling water is used as cooling media.

In process modification, it is desirable to reuse the existing heat exchangers as much as possible. Therefore, the UA of heat exchangers were analyzed to see that which heat exchangers could be reused. If the value of heat exchanger UA is greater than the value required in modification, then heat exchangers can be reused in modification. The result of UA analysis is shown in Table 4.10.

Table 4.10 UA analysis of heat exchangers

Heat Exchanger	Existing UA (MW/K)	Modified UA (MW/K)	Existing area (m ²)	Modified area (m ²)
Cold box 1	2.365	2.365	10083.600	10083.600
Cold box 2	0.876	0.876	5283.000	5283.000
Cold box 3	0.528	0.528	1918.700	1918.700
E70303	0.036	0.008	76.100	16.737
E70304	0.534	0.480	1539.000	1383.134
E70404	0.170	0.165	534.000	476.655
E70407	0.020	0.011	121.200	58.812
E70408	0.049	0.022	145.000	64.164
E70409	0.034	0.014	134.000	55.093
E70601	0.224	0.183	510.000	416.094
Total	4.836	4.651	20344.600	19755.989

From Table 4.10, it can be seen that the value of UA and heat transfer area of all existing heat exchangers are greater than that of the modified solution. Thus, no modification is required for the existing heat exchangers.

The heat exchanger network performances were compared between the current and modified network, which is shown in Table 4.11.

By comparing Tables 4.7 and 4.9, it can be seen that the utility exchanger's duty is reduced. In addition, the energy saving is made on the cooling

water. The economic analysis of modified heat exchanger network is shown in Table 4.12.

Table 4.11 Comparison of heat exchanger network performances between existing and modified network

Performances	Existing network	Modified network
Hot utility (MW)	0.00	0.00
Cold utility (MW)	12.18	7.80
Number of heat exchangers		
Shell and tubes	7	7
Cold boxes	3	3
Total area (m ²)	20,344.60	20,344.60

Table 4.12 Economic analysis of modified heat exchanger network

Economic index	Saving (US\$/yr.)	Investment (US\$)	PBP* (yr.)	IRR** (%)
Network	71,018.60	0.00	0.00	-

* PBP = Payback period = (investment)/(saving)

**IRR = Internal rate of return

The detail calculation for economic analysis is summarized in Appendix C. It can be seen from Table 4.12 that the operating cost saving for modified network (US\$ 71,018.60 / yr.) is less than that was predicted (US\$ 1,362,092.40 / yr.). The reason is that the network energy reduction was done mostly on cooling water. Since the price of cooling water (US\$ 0.0009/kW-hr.) is cheaper than the price of refrigerant (US\$ 0.0355/ kW-hr.), therefore, the energy saving is less than that was predicted.

In summary, the modified heat exchanger network can save energy 36.07 % compared to the existing one. The condition of heat exchangers was

changed a little bit from the design value, without modifications, but it can result in substantially saving in utility consumption (US\$ 71,018.60/yr.)

4.5 Exergy analysis

In this study, the exergy analysis was conducted twice. The first analysis was done for the gas separation plant unit I before modification. Another analysis was done for the gas separation plant unit I after the modification. The detail calculation is shown in Appendix D. It was shown that the stream exergy is mostly thermal exergy. The result for the first and second analysis are compared and shown in Figure 4.25 and 4.26, respectively.

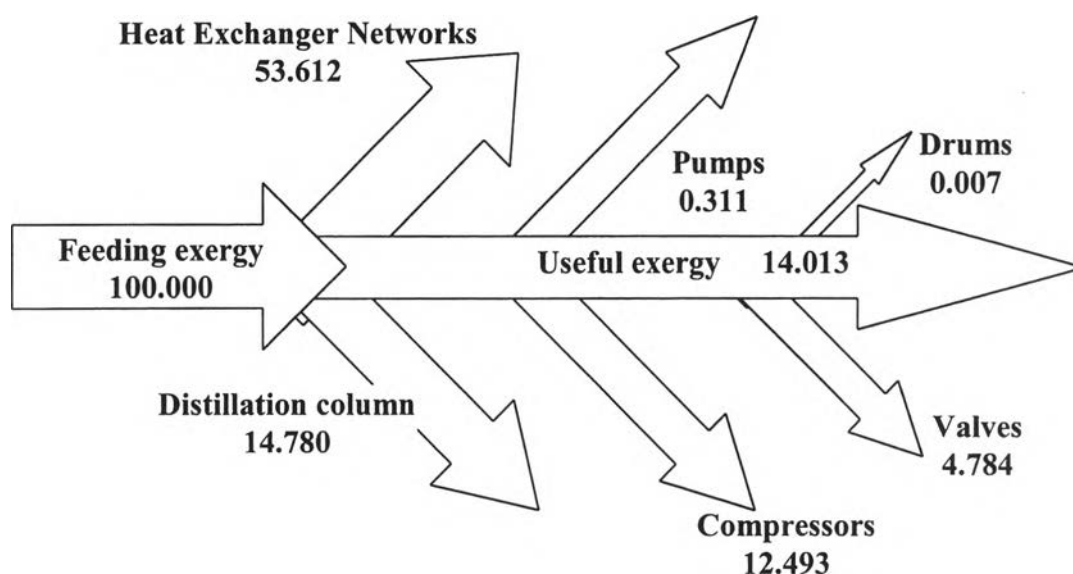


Figure 4.25 Exergy analysis of gas separation process before modification.

From Figure 4.25, it can be seen that the exergy was mostly lost on heat exchanger networks. Exergy loss in heat exchanger network is 53.612 %, from the feeding exergy. However, when the heat exchanger network was modified, the exergy loss in heat exchanger network was reduced from 53.612 % to 52.082 %. The exergy loss does not only reduced in heat exchanger network, as shown in Figure 4.26, the exergy loss in distillation column, compressor, valve, flash drum,

and pumps also reduced. This results in more useful work in the process, which increases the thermodynamic efficiency.

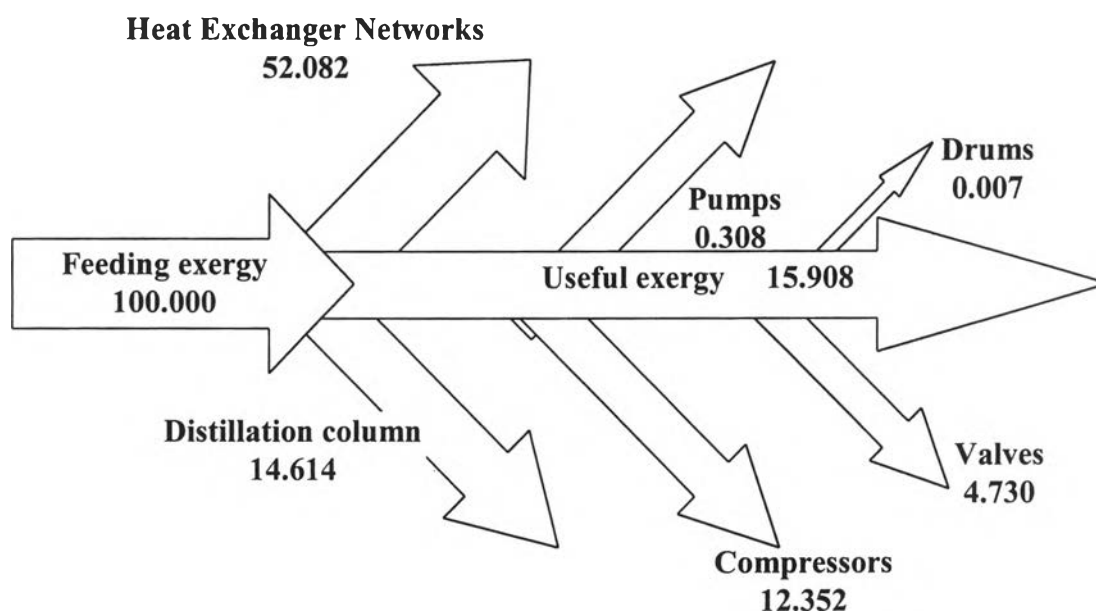


Figure 4.26 Exergy analysis of gas separation process after modification.

The useful work in this case is the work that is required to separate natural gas into various products; i.e., sale gas, ethane, propane, LPG, and natural gasoline. The percentage exergy loss in each equipment and exergetic efficiency for both before and after modification were summarized in Table 4.13. It can be seen that the exergy loss in heat exchanger network was reduced from 53.612 to 52.082 % and the exergetic efficiency increased from 14.013 % to 15.908 %. Thus, the heat exchanger network modification can reduce the process exergy loss and therefore, increase exergetic efficiency. This can be concluded that the heat exchanger network modification by pinch technology can improve thermodynamic efficiency of the process.

Table 4.13 Percentage exergy loss by equipment for both before and after modification

Equipment	Before modification	After modification
Distillation columns	14.780	14.614
Heat Exchanger Networks	53.612	52.082
Flash drums	0.007	0.007
Valves	4.784	4.730
Expanders	0.000	0.000
Compressors	12.493	12.352
Pumps	0.311	0.308
Exergetic efficiency	14.013	15.908